

Chapter 3

Electromagnetic transition form factors of light pseudoscalar mesons

When an elementary particle couples to the photon, its coupling can be determined by a few dimensionless parameters, for example, its total charge and magnetic moment. But, the case of composite particles is different in the sense that these coefficients must be replaced by momentum dependent functions known as "the form factors". These functions describe the distribution of charge and current inside a particle, hence, reveal its internal structure. Experimental and theoretical studies of form factors of hadrons are of major importance as they aim to answer many fundamental questions like how to understand the differences within mesons and baryons forming multiplets in $SU(3)_f$ representation. What happens to hadron when very high energy being pumped on it from outside? How far the models based on quantum chromodynamics are successful in explaining the experimental data of form factors? For proton and other nuclei, which are available as targets, the form factors are studied from elastic scattering experiments. But other baryons and mesons which are not available as targets, the information on form factors come from the electron-positron colliders [92–97]. Among all hadrons, the studies of form factors involving mesons are considered to be simpler and insightful as they possess less complexity than baryons in terms of their quark structure. In chapter 1, we have stated many reasons that explain why the rigorous studies on aspects involv-

ing pseudoscalar mesons, particularly η and η' , are essential. In this chapter, we are going to describe studies on electromagnetic Transition Form Factors (TFFs) of these mesons.

To probe a structure of any hadron, usually, a photon is used and we get electromagnetic form factors of hadron of interest. For π^0, η and η' , C-invariance implies that electromagnetic form factor is identically zero for all Q^2 . Therefore, to probe the structure of these mesons, a different reaction is required and the process $\gamma\gamma^* \rightarrow P$ TFFs provides a good option. The main process here is, $e^+e^- \rightarrow e^+e^-P, P = \pi^0, \eta, \eta'$ where the final state P is produced via two-photon production mechanism shown in Fig. (3.1). Rigorous studies on these processes not only provide information about the quark-gluon structure of mesons in question but also test models based on QCD. Furthermore, the mechanism responsible for the large masses of some of these mesons may also manifest its outcome in the processes that study TFFs. The TFFs of light pseudoscalar mesons have remained a subject of much experimental [92–97] and theoretical [37, 38, 40, 41, 46, 98–108] interest since past few decades.

3.1 A glimpse on some studies of electromagnetic transition form factors of light pseudoscalar mesons

The differential cross-section $\frac{d\sigma(e^+e^- \rightarrow e^+e^-P)}{dQ^2}$ of the pseudoscalar meson production process $e^+e^- \rightarrow e^+e^-P$ depends on the quantity $F_{\gamma^*\gamma \rightarrow P}(Q^2)$ (TFF), which describes $\gamma^*\gamma \rightarrow P$ transition. This exclusive reaction though involves large momentum transfer, the properties of transition form factors depend essentially both on perturbative interactions which warrant the large momentum transfer and on the non-perturbative ones which are behind the hadron formation out of quarks and gluons. Thus, in order to determine not only the energy dependence but also the absolute values of the amplitudes, one should be able to calculate both hard perturbative part of the amplitude and the non-perturbative hadronic wave functions. The tran-

sition form factors cannot be calculated directly from QCD analytically, hence the theoretical investigations rely upon pQCD, QCD sum rules, and other theoretical methods.

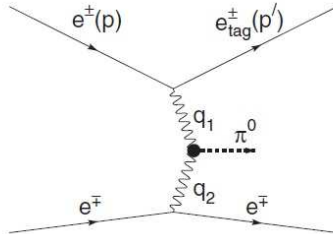


Figure 3.1: The Feynman diagram for the $e^+e^- \rightarrow e^+e^-\pi^0$ process

3.1.1 pQCD and TFFs of light pseudoscalar mesons

Due to "anti-screening" of charges in QCD, the possibility to calculate the interactions efficiently at short-distances arises with the assistance of the perturbation theory. This led to considerable progress in our understanding of the exclusive processes. pQCD calculations combined with the available parametrization of the non-perturbative processes enables us to understand a large set of data from high-energy reactions.

One of the important aspects of pQCD based methods is a factorization procedure [100] that separates perturbative short-distance effects from non-perturbative long-distance ones. The Transition Form Factors (TFFs) are expressed as a convolution of hard scattering amplitude (calculable parton-parton process) with the soft non-perturbative wave function of a meson. The latter, however, cannot be calculated from pQCD, their evolution with the scale(Q^2) is calculable [99, 100]. Factorization thus separates rapid hard scattering from the slower time scale of non-perturbative processes such as quark-fragmentation. The fundamental framework that lies behind factorization theorems used in investigating exclusive processes is the operator product expansion (OPE) near the light-cone [5, 37]. In this, the product of two

currents is written as [5],

$$j(x)j(0) = \sum_{i,n} C_n^{(i)}(x^2)x^{\mu_1} \dots x^{\mu_n} \mathcal{O}_{\mu_1, \dots, \mu_n}^{(i)}(0), \quad (3.1)$$

where i distinguishes operators by their type and n is the spin of the operator. Eq. (1.31) of Chapter 1, also shows the product of two currents but there lies an important difference between these two. The above equation is essentially an expansion near the light cone, $x^2 \sim 0$ rather than $x \sim 0$ (short-distance expansion). The short-distance expansion corresponds to large q region where $|q^2| \gg |p \cdot q|, |p^2|, m^2$ and in physical applications, we have to deal with the situations where $|q^2| \sim |p \cdot q| \gg |p^2|, m^2$ in the scattering process. Then, we need to use light-cone expansion. In Eq. (3.1), $C_n^{(i)}(x^2)$ are singular c-number coefficients. The singularity structure of these functions is important in making physical predictions of the process. $\mathcal{O}_{\mu_1, \dots, \mu_n}^{(i)}(0)$ are non-singular local operators. To determine the structure of singularity in free-field theory, the dimensional counting is used [5],

$$C_n^{(i)}(x^2) \sim (x^2)^{-d_{j_0} - n/2 + d_o^i(n)/2}, \quad (3.2)$$

where d_{j_0} and $d_o^i(n)$ are canonical dimensions of $j(x)$ and $\mathcal{O}_{(\mu_1, \dots, \mu_n)}^i$ respectively. The strength of singularity then determined by the difference $d_o^i(n) - n$, called as the twist of a composite operator.

$$\tau_n^i \equiv d_o^i(n) - n. \quad (3.3)$$

The expansion is done in terms of operators of an increasing twist. The lowest twist operators dominate in the light-cone expansion and give the most singular contribution. The above equation, however, gets modified in the case of interacting fields where the canonical dimensions of operators are replaced by scale dimensions d_j and $d^i(n)$.

$$C_n^{(i)}(x^2) \sim (x^2)^{-d_j - n/2 + d^i(n)/2}, \quad (3.4)$$

Thus, the 'twist' of a composite operator becomes an essential feature of light-cone expansion and the dimension is not the only one which determines the importance

of an operator but rather the difference between the dimension and the spin of an operator, the twist, which determines the dominance of an operator.

Brodsky and Lepage employed pQCD to find the asymptotic behavior of the $\gamma\gamma^* \rightarrow P$ TFFs in the limit of $Q^2 \rightarrow \infty$ [100],

$$\lim_{Q^2 \rightarrow \infty} Q^2 F_{\gamma^* \gamma P}(Q^2) = 2f_P, \quad (3.5)$$

It has been predicted that in this limit any mesonic wave function evolves to the asymptotic wave function of the unique shape. The behaviour of TFF in the limit $Q^2 \rightarrow 0$ can be determined from the axial anomaly in the chiral limit of QCD. For π^0 and η , the axial anomaly yields [102],

$$\lim_{Q^2 \rightarrow 0} Q^2 F_{\gamma^* \gamma P}(Q^2) = \frac{1}{4\pi^2 f_P}, \quad (3.6)$$

to leading order in $\frac{m_u^2}{m_P^2}$ and $\frac{m_d^2}{m_P^2}$. However, this prediction does not hold good for η' due to associated axial anomaly and larger value of s-quark mass. For intermediate value of Q^2 between $Q^2 \rightarrow 0$ and $Q^2 \rightarrow \infty$, a simple interpolation has been proposed [102]

$$Q^2 F_{\gamma^* \gamma \rightarrow \pi^0}(Q^2) \sim \frac{1}{4\pi^2 f_P} \frac{1}{1 + \left(\frac{Q^2}{8\pi^2 f_P^2}\right)}, \quad (3.7)$$

Thus, in the earliest research works [99–101], pQCD was considered to predict the behaviour of form factor at the boundaries. In [41], QCD corrections to the hard scattering amplitude(T_H) were calculated using dimensional regularization.

3.1.2 The pion's case

Pion, being the simplest hadron, its TFF has been studied widely. In pion's case, the 'soft' contributions to the leading order either do not exist or they are suppressed thus making the situation simpler for the testing of QCD factorization approach. Pion DAs are also used to describe other hard exclusive reactions. From the factorization theorem, the TFF (to leading order in QCD coupling constant)for pion can

be written as,

$$F_{\gamma^*\gamma\rightarrow\pi^0}(Q^2) = \frac{\sqrt{2}f_\pi}{3} \int_0^1 dx T_H(x, Q^2, \mu, \alpha_s(\mu)) \phi_\pi(x, \mu), \quad (3.8)$$

where f_π is pion decay constant, x is the fraction of momentum carried by a quark or antiquark in the pion, T_H is the hard scattering amplitude for the process $\gamma\gamma^* \rightarrow q\bar{q}$, μ is the renormalization scale and ϕ_π is the leading-twist pion distribution amplitude (DA).

The distribution amplitude $\phi_\pi(x, \mu)$, appearing in Eq.(3.8) is purely perturbative only in the asymptotic limit $Q^2 \rightarrow \infty$ i.e $\phi_\pi(x, \mu \rightarrow \infty) \rightarrow \phi_{as}(x)$. In this limit, the form of distribution amplitude becomes independent of the properties of the hadron involved. But, at experimentally accessible momentum transfer ($10GeV^2 \leq |Q^2| \leq 100GeV^2$), its form differs very much from the asymptotic one as its evolution with Q^2 is very mild. Then, one cannot use pQCD to investigate its properties. Therefore, to extract an information on its properties, non-perturbative methods like QCD sum rules [37], Lattice QCD [109], light cone sum rules [110, 111] were used to calculate the first few moments of pion distribution amplitude. ϕ_π is defined by the matrix element of the nonlocal quark-antiquark operator separated by light-like distances [40]

$$\langle 0 | \bar{q}(0)[0, \alpha n] \not{n} \gamma_5 q(\alpha n) | \pi^+(p) \rangle = i f_\pi p \cdot n \int_0^1 dx e^{-ix\alpha p \cdot n} \phi_\pi(x, \mu), \quad (3.9)$$

where

$$[0, \alpha n] = P e^{-ig \int_0^\alpha du n^\mu A_\mu(un)}, \quad (3.10)$$

Above equation represents path-order gauge link which absorbs all gluon attachments to the hard subgraph. From renormalization group(RG) equations, the expansion of pion DA can be done in terms of Gegenbauer polynomials.

$$\phi_\pi(x, \mu) = \sum_{n=0}^{\infty} a_n(\mu) \phi_n(x), \quad (3.11)$$

where $\phi_n(x) = 6x(1-x)C_n^{3/2}(2x-1)$ and $C_2^{1/2}(t) = \frac{1}{2}(3t^2 - 1)$, $C_2^{3/2}(t) = \frac{3}{2}(5t^2 - 1)$, $C_1^{5/2}(t) = 5t$, etc [99, 100]. The normalization condition, $\int_0^1 dx \phi_\pi(x, \mu) = 1$ fixes

the first coefficient $a_0(\mu) = 1$ and remaining coefficients have to be calculated by using non-perturbative methods or extracted from experimental data.

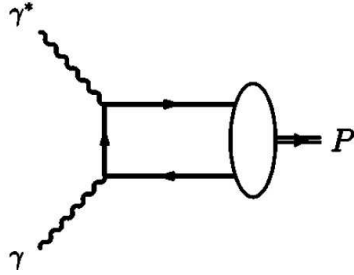


Figure 3.2: Lowest order Feynman diagram for $\gamma^*\gamma \rightarrow P, P = \pi^0, \eta, \eta'$.

Experimental measurements of the Transition Form Factors of π^0, η and η' was first done by CELLO [92] collaboration. The form factors of π^0, η were measured in the range $Q^2 < 2.5\text{GeV}^2$ and of η' in $Q^2 \leq 7\text{GeV}^2$. CLEO [93] measured $F_{\gamma^*\gamma}$ in the space-like region of $1.5 \leq Q^2 \leq 9\text{GeV}^2$ for π^0 , $1.5 \leq Q^2 \leq 20\text{GeV}^2$ for η and $1.5 \leq Q^2 \leq 30\text{GeV}^2$ for η' . The experimental data and pQCD predictions were proved to be consistent with each other. BABAR in 2006 [94] measured TFF for $e^+e^- \rightarrow \eta^{(\prime)}\gamma$ at time-like momentum transfer $q^2 = 112\text{GeV}^2$. This measurement concluded no tension with the theory but pointed out that more theoretical input is needed to get precise results consistent with the data in $\eta - \eta'$'s case, as they involve some peculiarities due to mixing, possible glue content, uncertainties in quark distribution amplitudes. When BABAR in 2009 [95], measured the $\pi^0\gamma^*\gamma$ TFF in a range $4 \leq Q^2 \leq 40\text{GeV}^2$, the disagreement arose between the proposed theoretical models on pion wave-functions and the experimental data. The scaling behaviour of form factor in the Q^2 range 20 GeV^2 to 40 GeV^2 , was not as predicted by pQCD. Reliable estimation of form factor by considering higher-order pQCD and power corrections thus became essential. The measured form factor for $Q^2 > 10\text{GeV}^2$ exceeded the estimate predicted by pQCD in the asymptotic limit, $Q^2 F(Q^2) = \sqrt{2}f_\pi \simeq 0.185\text{GeV}$ for $Q^2 \rightarrow \infty$. The NLO power corrections due to twist-four contribution to $\pi^0\gamma^*\gamma$ TFF calculated in [112], are found to be reliable only for $Q^2 > 15\text{GeV}^2$. What would be an effect of yet higher order power corrections coming

from twist-6, was an important question to address. In [40], twist-six contributions to the electromagnetic transition form factor of pion has been calculated in LCSR approach and they were found to be substantial.

The twist-six contribution to pion transition form factor corresponds to OPE of the product of two electromagnetic currents involving twist-six four-quark pion DA in the factorization method. One quark-antiquark pair forms a condensate and other one forms a twist-three quark-antiquark DA. This twist-three DAs are parameterized as [82],

$$\langle 0 | \bar{q}(0) i \gamma_5 q(\alpha n) | \pi(p) \rangle = \frac{f_\pi m_\pi^2}{m_u + m_d} \int_0^1 dx e^{-ix\alpha pn} \phi_{3\pi}^p(x), \quad (3.12)$$

$$\langle 0 | \bar{q}(0) i \sigma_{\mu\nu} \gamma_5 q(\alpha n) | \pi(p) \rangle = \frac{i}{6} (p_\mu x_\nu - p_\nu x_\mu) \frac{f_\pi m_\pi^2}{(m_u + m_d)} \int_0^1 dx e^{-ix\alpha pn} \phi_{3\pi}^\sigma(x), \quad (3.13)$$

The contribution coming from these DAs which is found to be suppressed when both photons are highly off-shell is no longer suppressed if one of the photons goes on mass shell i.e $q^2 \rightarrow 0$. In fact, it leads to singularity in the calculation and has to be regulated by replacing $1/q^2 \rightarrow 1/(m_\rho^2 + q^2)$. This approach is known as vector-meson dominance approximation where the transition of photon to meson occurs through the ρ -meson, which has the same quantum numbers as photon. The regulator $1/m_\rho^2$ is identified as the magnetic susceptibility of the quark-condensate [83, 113, 114]. Thus, twist-six calculations done in [40] proved that contributions coming from higher twists may be non-negligible as soft non-perturbative corrections play the role.

3.1.3 The case of η and η'

Extensive theoretical and experimental studies on electromagnetic transition form factors of η and η' have been done in the past due to many interesting features of these particles. $\eta - \eta'$ mixing, the admixture of gluon component in the singlet reflecting into the mixing of singlet distribution amplitude with gluon distribution

amplitude under evolution, their association with the axial U(1) anomaly [115] are peculiar phenomena which make the studies on these TFFs much more attentive. To leading order, the $\eta\gamma$ and $\eta'\gamma$ TFFs are purely electromagnetic but at Next-to-leading order (NLO), the gluon components in η and η' contribute directly. Furthermore, these gluon components can also affect the result at LO as the DAs evolve.

$\eta - \eta'$ mixing and the decay constants

As discussed in Chapter 1, there are two equivalent ways through which $\eta - \eta'$ mixing is described. In Chapter 1, we have described its main aspects and a few important equations are also given. Eqs.(1.20) and (1.21) show the relation between $f_M^i (i = 1, 8, q, s)$ and basic decay constants. The decay constants probe the quark distributions at zero spatial separation and in the case of $\eta - \eta'$, the mixing of meson states involve global wavefunctions (large distance effect) and the mixing of decay constants involve short-distance effect. Because of flavor symmetry breaking the mixing of the decay constants can be identical to the mixing of particle states at most for a specific choice of the basis. Theoretical and phenomenological investigations show that the quark flavor basis possess this property and thus reduces number of mixing parameters. Introducing,

$$a_M = \langle M(p) | \frac{\alpha_s}{4\pi} G_{\mu\nu}^a \tilde{G}^{a\mu\nu} | 0 \rangle, \quad (3.14)$$

$$h_M^q = 2im_q \langle M(p) | \frac{1}{\sqrt{2}} (\bar{u}\gamma_5 u + \bar{d}\gamma_5 d) | 0 \rangle, \quad (3.15)$$

$$h_M^s = 2im_s \langle M(p) | \bar{s}\gamma_5 s | 0 \rangle, \quad (3.16)$$

one finds,

$$a_M = \frac{1}{\sqrt{2}} (h_M^q - f_M^q m_M^2) = h_M^s - f_M^s m_M^2, \quad (3.17)$$

where $m_q = (m_u + m_d)/2$.

The decay constants in singlet-octet basis are related to those in QF basis as follows,

$$f_\eta^{(q)} = f_q \cos \phi = \frac{1}{\sqrt{3}}(\sqrt{2}f_\eta^0 + f_\eta^8), \quad (3.18)$$

$$f_\eta^{(s)} = -f_s \sin \phi = \frac{1}{\sqrt{3}}(f_\eta^0 - \sqrt{2}f_\eta^8), \quad (3.19)$$

$$f_{\eta'}^{(q)} = f_q \sin \phi = \frac{1}{\sqrt{3}}(\sqrt{2}f_{\eta'}^0 + f_{\eta'}^8), \quad (3.20)$$

$$f_{\eta'}^{(s)} = f_s \cos \phi = \frac{1}{\sqrt{3}}(f_{\eta'}^0 - \sqrt{2}f_{\eta'}^8). \quad (3.21)$$

The constants $f_{3q,3s}$ are three-particle decay constants which appear in twist-3 three-particle DAs $\Phi_{3M}^{(i)}$. They are introduced in analogy with $f_{3\pi}$ as follows:

$$\langle M(p) | \frac{1}{\sqrt{2}}(\bar{u}(0)\sigma_{z\mu}\gamma_5 G^{z\mu}u(0) + \bar{d}(0)\sigma_{z\mu}\gamma_5 G^{z\mu}d(0)) | 0 \rangle = 2i(p.z)^2 f_{3M}^{(q)}, \quad (3.22)$$

$$\langle M(p) | \bar{s}(0)\sigma_{z\mu}\gamma_5 G^{z\mu}s(0) | 0 \rangle = 2i(p.z)^2 f_{3M}^{(s)}. \quad (3.23)$$

$G_{\mu z} = G_{\mu\xi}z^\xi$ and z^ξ is a light-like vector.

The distribution amplitudes

Distribution amplitudes describe the momentum fraction distributions of partons in a meson, in a particular Fock state, with a fixed number of constituents. The leading-twist (twist-two) DAs $\Phi_M^{(i)}(u, \mu)$ at a given scale μ , are defined in terms of matrix elements of bilocal quark currents as,

$$\langle M(p) | \frac{1}{\sqrt{2}}(\bar{u}(z_2)\gamma_\mu\gamma_5 u(z_1) + \bar{d}(z_2)\gamma_\mu\gamma_5 d(z_1)) | 0 \rangle = -if_M^{(q)} p_\mu \int_0^1 du e^{i(up.z_2 + \bar{u}p.z_1)} \Phi_M^{(q)}(u, \mu) + \dots, \quad (3.24)$$

$$\langle M(p) | \bar{s}(z_2)\gamma_\mu\gamma_5 s(z_1) | 0 \rangle = -if_M^{(s)} p_\mu \int_0^1 du e^{i(up.z_2 + \bar{u}p.z_1)} \Phi_M^{(s)}(u, \mu) + \dots \quad (3.25)$$

The leading twist DA which describes the momentum distribution of the valence quarks in the meson, is related to the meson's Bethe-Salpeter wave function ϕ_{BS} by [82],

$$\phi(x) \sim \int^{|k_\perp| < \mu} d^2 k_\perp \phi_{BS}(x, k_\perp). \quad (3.26)$$

Here μ denotes the separation scale between perturbative and non-perturbative regime. In above equations as well as in the following, path-ordered gauge connection between non-local quark (gluon) operators [37, 38, 40, 46, 82, 98, 103–106] is understood. Thus, in Eqs. (3.24) and (3.25), on L.H.S, there exists a factor,

$$[z_2, z_1] = \mathcal{P}e^{(ig \int_{z_1}^{z_2} dz^\mu A_\mu^n(z) t^n)} \quad (3.27)$$

between the two quark fields to ensure gauge invariance of the bilocal axial-vector quark operators. In Eq. (3.27), \mathcal{P} stands for path ordering, g is the QCD coupling constant, $A_\mu^n(z)$ is a four-potential of the gluonic field, t^n are the generators of the colour SU(3) group and the integration is performed over the straight line connecting the points z_1 and z_2 . Left out terms on the R.H.S of Eqs. (3.24) and (3.25) are either of higher twists or of higher order in the light-cone expansion. u and $\bar{u} = (1 - u)$ are the momentum fractions carried by the quark and the antiquark inside the meson. The gluonic twist-two DAs are defined as [104],

$$\langle M(p) | G_{\mu z}(z) \tilde{G}^{\mu z}(-z) | 0 \rangle = \frac{1}{2} (p \cdot z)^2 \frac{C_F}{\sqrt{3}} f_M^0 \int_0^1 du e^{ip \cdot z(2u-1)} \Phi_M^{(g)}(u, \mu), \quad (3.28)$$

$\tilde{G}^{\mu z}$ is dual gluon field tensor, $C_F = \frac{4}{3}$ and f_M^0 is the singlet current decay constant. $\Phi_M^{(g)}(u)$ is antisymmetric under $u \leftrightarrow \bar{u}$. The twist-two DAs for quark-antiquark components and gluonic ones can be expanded in terms of Gegenbauer polynomials $C_n^{3/2}(2u - 1)$ and $C_{n-1}^{5/2}(2u - 1)$ as [84, 103, 104],

$$\Phi_M^{(i)}(u, \mu) = 6u\bar{u} \left(1 + \sum_{n=2,4,..} B_n^{M,i}(\mu) C_n^{3/2}(2u - 1) \right), \quad (i = q, s), \quad (3.29)$$

$$\Phi_M^{(g)}(u, \mu) = u^2\bar{u}^2 \sum_{n=2,4,..} B_n^{M,g}(\mu) C_{n-1}^{5/2}(2u - 1). \quad (3.30)$$

The quark distribution amplitudes are symmetric under $u \rightarrow (1-u)$ and $\int_0^1 du \phi_{P_i}(u, \mu_F^2) = 1$. The gluon distribution amplitude is antisymmetric and $\int_0^1 du \phi_{P_g}(u, \mu_F^2) = 0$. Higher twist DAs include either contributions of components with "wrong" spin projection or contributions of transverse motion of quarks (antiquarks) in the leading twist components. They also account for contributions of higher Fock states

with additional gluons and/or quark-antiquark pairs [82].

Because the gluon and flavor singlet quark DAs mix under evolution, the gluon DA is usually assigned the same factor as flavor singlet quark DA. The mixing equation has a 2×2 matrix form which has been solved [38, 103, 105]. Keeping only the first non-asymptotic term in the singlet component of the twist-two DAs, the quark-antiquark and gluon DAs can be written as

$$\Phi_{\eta_0}^{(q)}(u, \mu^2) = 6u\bar{u}[1 + A(\mu^2) - 5A(\mu^2)u\bar{u}], \quad (3.31)$$

$$\Phi_{\eta_0}^{(g)}(u, \mu^2) = u^2\bar{u}^2(u - \bar{u})B(\mu^2). \quad (3.32)$$

For $n_f=4$, the functions $A(\mu^2)$ and $B(\mu^2)$ are given by [38, 105],

$$A(\mu^2) = 6B_2^q L^{\frac{48}{75}}(\mu^2) - \frac{B_2^g}{17} L^{\frac{107}{75}}(\mu^2), \quad (3.33)$$

$$B(\mu^2) = 19B_2^q L^{\frac{48}{75}}(\mu^2) + 5B_2^g L^{\frac{107}{75}}(\mu^2), \quad (3.34)$$

where $\mu_0^2 = 1\text{GeV}^2$ is a normalization scale, coefficients B_2^q and B_2^g are introduced in Eqs. (3.29) and (3.30) and

$$L(\mu^2) = \frac{\alpha_s(\mu^2)}{\alpha_s(\mu_0^2)}. \quad (3.35)$$

The DA of octet state has only the quark component $\Phi_{\eta_8}(u, \mu^2)$ where $C(\mu^2)$ replaces $A(\mu^2)$:

$$C(\mu^2) = 6B_2^q L^{2/3}. \quad (3.36)$$

Two-particle twist-3 DAs $\Phi_{3M}^{(i)p,\sigma}(u)$ are introduced as follows [82, 98, 103]:

$$2m_q \langle M(p) | \frac{1}{\sqrt{2}} (\bar{u}(z_2) i\gamma_5 u(z_1) + \bar{d}(z_2) i\gamma_5 d(z_1)) | 0 \rangle = \int_0^1 du e^{i(up.z_2 + \bar{u}p.z_1)} \Phi_{3M}^{(q)p}(u), \quad (3.37)$$

$$2m_s \langle M(p) | (\bar{s}(z_2) i\gamma_5 s(z_1)) | 0 \rangle = \int_0^1 du e^{i(up.z_2 + \bar{u}p.z_1)} \Phi_{3M}^{(s)p}(u), \quad (3.38)$$

$$2m_q \langle M(p) | \frac{1}{\sqrt{2}} (\bar{u}(z_2) \sigma_{\mu\nu} \gamma_5 u(z_1) + \bar{d}(z_2) \sigma_{\mu\nu} \gamma_5 d(z_1)) | 0 \rangle = \frac{i}{6} (p_\mu z_\nu - p_\nu z_\mu) \int_0^1 du \times e^{i(up.z_2 + \bar{u}p.z_1)} \Phi_{3M}^{(q)\sigma}(u) \quad (3.39)$$

$$2m_s \langle M(p) | (\bar{s}(z_2) \sigma_{\mu\nu} \gamma_5 s(z_1)) | 0 \rangle = \frac{i}{6} (p_\mu z_\nu - p_\nu z_\mu) \int_0^1 du e^{i(up \cdot z_2 + \bar{u}p \cdot z_1)} \Phi_{3M}^{(s)\sigma}(u), \quad (3.40)$$

where $z = z_2 - z_1$. These twist-three DAs are normalized as:

$$\int_0^1 du \Phi_{3M}^{(q)p}(u) = \int_0^1 du \Phi_{3M}^{(q)\sigma}(u) = h_M^{(q)}, \quad (3.41)$$

$$\int_0^1 du \Phi_{3M}^{(s)p}(u) = \int_0^1 du \Phi_{3M}^{(s)\sigma}(u) = h_M^{(s)}. \quad (3.42)$$

We follow the following parameterization of these DAs [98]:

$$\begin{pmatrix} \Phi_{3\eta}^{(q)p,\sigma} & \Phi_{3\eta}^{(s)p,\sigma} \\ \Phi_{3\eta'}^{(q)p,\sigma} & \Phi_{3\eta'}^{(s)p,\sigma} \end{pmatrix} = U(\phi) \begin{pmatrix} \Phi_{3q}^{p,\sigma} & 0 \\ 0 & \Phi_{3s}^{p,\sigma} \end{pmatrix}, \quad (3.43)$$

where $U(\phi)$ is the same matrix as used in parameterizing $f_M^{(i)}$.

These DAs are expanded in terms of Gegenbauer polynomials as [98],

$$\Phi_{3q}^p(u) = h_q + 60m_q f_{3q} C_2^{1/2}(2u-1) + \dots, \quad (3.44)$$

$$\Phi_{3s}^p(u) = h_s + 60m_s f_{3s} C_2^{1/2}(2u-1) + \dots, \quad (3.45)$$

$$\Phi_{3q}^\sigma(u) = 6u\bar{u} \left(h_q + 10m_q f_{3q} C_2^{3/2}(2u-1) + \dots \right), \quad (3.46)$$

$$\Phi_{3s}^\sigma(u) = 6u\bar{u} \left(h_s + 10m_s f_{3s} C_2^{3/2}(2u-1) + \dots \right). \quad (3.47)$$

Constants are parameterized as,

$$\begin{pmatrix} h_\eta^{(q)} & h_\eta^{(s)} \\ h_{\eta'}^{(q)} & h_{\eta'}^{(s)} \end{pmatrix} = U(\phi) \begin{pmatrix} h_q & 0 \\ 0 & h_s \end{pmatrix}, \quad (3.48)$$

$$\begin{pmatrix} f_{3\eta}^{(q)} & f_{3\eta}^{(s)} \\ f_{3\eta'}^{(q)} & f_{3\eta'}^{(s)} \end{pmatrix} = U(\phi) \begin{pmatrix} f_{3q} & 0 \\ 0 & f_{3s} \end{pmatrix}. \quad (3.49)$$

The three-particle twist-three DA is defined as [81, 116],

$$\begin{aligned} \langle M(p) | \bar{r}(x) g G_{\mu\nu}^m(vx) \frac{\lambda^n}{2} \sigma_{\alpha\beta} \gamma_5 r(0) | 0 \rangle &= i f_{3M}^{(r)} [(p_\mu p_\alpha g_{\nu\beta} - p_\nu p_\alpha g_{\mu\beta}) - (p_\mu p_\beta g_{\nu\alpha} - p_\nu p_\beta g_{\mu\alpha})] \times \\ &\int_0^1 d\alpha_1 d\alpha_2 d\alpha_3 \delta(1 - \alpha_1 - \alpha_2 - \alpha_3) \Phi_{3M}^{(r)}(\alpha_1, \alpha_2, \alpha_3) e^{ipx(\alpha_1 + v\alpha_3)} \end{aligned} \quad (3.50)$$

where $r=q, s$, $0 \leq v \leq 1$, $f_{3q} \approx f_{3s} \approx f_{3\pi}$ and

$$\Phi_{3M}^{(r)}(\alpha_1, \alpha_2, \alpha_3) = 360\alpha_1\alpha_2\alpha_3^2 \{ 1 + \lambda_{3r}(\alpha_1 - \alpha_2) + \omega_{3r} \frac{1}{2}(7\alpha_3 - 3) \}. \quad (3.51)$$

Combining Eqs. (1.21), (3.17) and (3.48) one obtains

$$h_q = f_q (m_\eta^2 \cos^2 \phi + m_{\eta'}^2 \sin^2 \phi) - \sqrt{2} f_s (m_{\eta'}^2 - m_\eta^2) \sin \phi \cos \phi. \quad (3.52)$$

Though h_q itself is small, the combination in which it normally appears is $\frac{h_q}{m_q}$, which is not small.

Electromagnetic TFFs of η and η' mesons

The electromagnetic TFF of η and η' is written as [46, 98, 104],

$$F_{M\gamma}(Q^2) = F_{M\gamma}^8(Q^2) + F_{M\gamma}^1(Q^2). \quad (3.53)$$

Both the flavor-octet and flavor singlet form factors can be written in terms of convolution of hard scattering amplitude and distribution amplitude, but the distribution amplitude in flavor-singlet form factor essentially carries two components: quark DA and the gluon DA. These DAs mix under evolution while the flavor-octet DA evolve independently with the scale. NLO hard scattering amplitudes for $\gamma^*\gamma \rightarrow q\bar{q}, gg$ subprocesses have been calculated in [104]. In the limit $Q^2 \rightarrow \infty$, transition form factor becomes,

$$F_{M\gamma} Q^2 \xrightarrow{Q^2 \rightarrow \infty} \frac{\sqrt{2} f_M^{eff}}{Q^2} \left[1 - \frac{5\alpha_s}{3\pi} \right] \quad (3.54)$$

where $f_P^{eff} \rightarrow \frac{1}{\sqrt{3}} [f_M^8 + 2\sqrt{2}f_M^1]$. The gluon contributions to $\eta\gamma$ and $\eta'\gamma$ electromagnetic TFFs are found to be subdominant in [38] but they are important for a wide range of exclusive processes like B-meson two-body nonleptonic exclusive and semi-exclusive decays involving η, η' . Furthermore, the gluonic effect is found to be negligible for η but sizable for η' . This result is obvious as the η and η' physical states consist of both the flavor $SU(3)_f$ octet η_8 and singlet η_1 states and $\eta_1\gamma$ TFF also contains gluonic part resulting into significant sensitiveness of $\eta'\gamma$ TFF to the gluonic contribution. The gluonic contribution to $B \rightarrow \eta, \eta'$ has been calculated in [117] and it was found to be negligible for η and significant for η' .

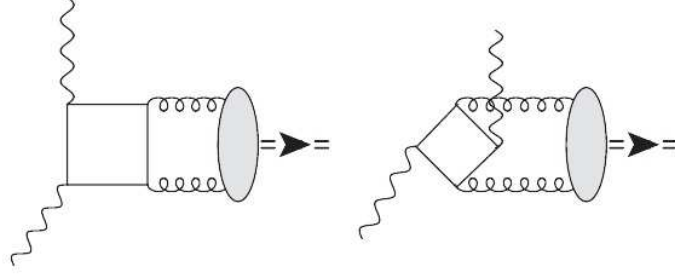


Figure 3.3: Diagrams contributing to gluonic coefficient function to $\eta\gamma, \eta'\gamma$ TFF

The Transition Form Factors of $\eta\gamma$ and $\eta'\gamma$ have been calculated in [46] by using well-known collinear factorization approach. This analysis was Next-to-leading order(NLO) in pQCD and a leading-twist in terms of power corrections. The argument was given that the leading-order theoretical analyses of these form factors are in accordance with the experimental results from CLEO [93] and L3 [118]. NLO leading-twist analysis [104] was found to be in reasonable agreement with these data. The authors in [104] have also compared their theoretical NLO, leading-twist results of $\eta\gamma$ and $\eta'\gamma$ to the BABAR [96] data with the assumption that the higher twist power-corrections are negligible. In the case of η, η' , one also has to choose the mixing scheme appropriately. In the calculation of TFF of these mesons, the inclusion of gluonic Fock state goes well with the singlet-octet basis. Gluonic admixture to singlet state can be understood easily than the complicated mixing with both $|q\bar{q}\rangle$ and $|s\bar{s}\rangle$ states separately. The authors in [46], had given the NLO expression for the transition form factor of $\eta - \eta'$ to leading-twist accuracy. The result reads,

$$\begin{aligned}
Q^2 F_{M\gamma} = & a_{M0}^{eff}(\mu_F) \left[1 - \frac{5\alpha_s \mu_R}{3\pi} \right] + a_{M2}^{eff}(\mu_F) \times \\
& \left[1 + \frac{5\alpha_s \mu_R}{3\pi} \left(\frac{59}{72} - \frac{5}{6} \log \frac{Q^2}{\mu_F^2} \right) \right] + a_{M4}^{eff}(\mu_F) \left[1 + \frac{5\alpha_s \mu_R}{3\pi} \left(\frac{10487}{4500} - \frac{91}{75} \log \frac{Q^2}{\mu_F^2} \right) \right] - \frac{20}{3\sqrt{3}} \frac{\alpha_s(\mu_R)}{\pi} f_M^1 \times \\
& \left[a_2^g(\mu_F) \left(\frac{55}{1296} - \frac{1}{108} \log \frac{Q^2}{\mu_F^2} \right) + a_4^g(\mu_F) \left(\frac{581}{10125} - \frac{7}{675} \log \frac{Q^2}{\mu_F^2} \right) \right].
\end{aligned} \tag{3.55}$$

where $n = 0, 2, 4, \dots$ and $a_0^i = 1$.

$$a_{Mn}^{eff}(\mu_F) = \sqrt{\frac{2}{3}} \left[f_M^8 a_n^8(\mu_F) + 2\sqrt{2} f_M^1 a_n^1(\mu_F) \right]. \tag{3.56}$$

For the plots, the authors had taken minimum value of $Q^2 = 2\text{GeV}^2$ and $\mu_0 = 1\text{GeV}$. Two-loop expression of α_s with four flavors $n_f = 4$ and with $\lambda_{\overline{MS}}^{(4)} = 0.319\text{GeV}$ had been used. $\mu_F = \mu_R = Q$ was kept in order to avoid $\log(\frac{Q^2}{\mu_F^2})$ terms. The series of Gegenbauer polynomials was truncated to $n = 2$ and different sets for Gegenbauer coefficients were taken. For an example, one set reads, $a_2^8 = -0.05 \pm 0.02$, $a_2^1 = -0.12 \pm 0.01$, $a_2^g = 19 \pm 5$. For other values of Gegenbauer coefficients one may refer [46].

Thus, the theory of η, η' electromagnetic TFFs is, on one hand, analogous to the QCD description of the $\pi^0\gamma$ TFF, it differs largely due to gluon-admixture, the contribution of heavy quarks and also due to large masses of η, η' . A theoretical framework of these TFFs had been updated in [98]. This calculation was done by using pQCD as well as light-cone sum rules(LCSR). The authors had also taken into account the c-quark contribution to gluon DA, strange quark mass and twist-four distribution amplitudes. To leading order in perturbation theory and considering twist-four corrections, the results were given as [98],

$$Q^2 F_{\gamma^*\gamma \rightarrow M}(Q^2) = 2 \sum_{\psi=u,d,s} e_\psi^2 F_M^{(\psi)} \left\{ 3(1 + C_{2,M}^{(\psi)}) - \frac{1}{Q^2} \left[\frac{h_M^{(\psi)}}{f_M^{(\psi)}} (2 + 3C_{2,M}^{(\psi)}) + \frac{80}{9} \delta_M^{2(\psi)} - \frac{h_M^{(\psi)}}{f_M^{(\psi)}} \left(\frac{67}{360} - \frac{5}{4} C_{2,M}^{(\psi)} \right) - \frac{3m_\psi f_{3M}^{(\psi)}}{2f_M^{(\psi)}} \right] \right\}. \quad (3.57)$$

where $H_M^{(u)} = H_M^{(d)} = h_M^{(q)}/\sqrt{2}$, $H_M^{(s)} = h_M^{(s)}$. One set of values of coefficients $C_{2,M}(\psi)$ reads, $C_2^{(q)} = 0.20$, $C_2^{(s)} = 0.20$, $C_4^{(q)} = 0.00$, $C_4^{(s)} = 0.00$, $C_2^{(g)} = -0.31$. General result for light-cone sum rules reads,

$$F_{\gamma^*\gamma \rightarrow M}^{LCSR}(Q^2) = F_{\gamma^*\gamma \rightarrow M}^{QCD}(Q^2) + \frac{1}{\pi} \int_0^{s_0} \frac{ds}{m_\rho^2} \left[e^{(m_\rho^2 - s)/M^2} - \frac{m_\rho^2}{s} \right] \text{Im} F_{\gamma^*\gamma \rightarrow M}^{QCD}(Q^2, -s). \quad (3.58)$$

The results in [98] imply that the higher-twist corrections do not have a large numerical impact. The pion electromagnetic TFF has been studied in [40] taking into account twist-6 corrections to it. We are going to describe twist-6 corrections to electromagnetic transition form factors of η and η' mesons within the collinear factorization approach.

3.2 Twist-six corrections to transition form factors of η and η' mesons

The content of this section and forthcoming sections is based on our work in [119]. From the previous sections, it is clear that the studies on TFFs of η and η' mesons are important in many ways. η and η' TFFs determine their quark-gluon structure and also fix their distribution amplitudes(DAs). These TFFs are also important ingredients for other processes such as the rates of rare decays $M \rightarrow l\bar{l}$ ($l = e, \mu$) [120], hadronic light-by-light scattering contribution to muon anomalous magnetic moment [121], $B \rightarrow \eta^{(\prime)}$ transition form factors [85, 122] and χ_{cJ} decays in pairs of η and η' mesons, etc. Since the theoretical studies based on pQCD have been done on these TFFs up to twist-four so far, we extend this calculation to twist-six. We calculate twist-six corrections to these TFFs using the well-known collinear factorization approach [100] in which TFFs get factorized into two parts: One is perturbation-theory friendly hard-scattering amplitude and the other is the universal meson Distribution Amplitude (DA) which includes non-perturbative dynamics of QCD bound states. The core essence of the factorization theorem is that all the short-distance dependence is there in the coefficient functions, while all long-distance dependence resides in the parton distribution amplitudes. The coefficient functions are infrared safe, and may be calculated perturbatively and corrections to factorization are suppressed by a power of Q^2 . These TFFs can also be calculated in approaches like k_T -factorization [123], anomaly sum rules [124] and some other approaches which do not directly hinge on QCD: namely, non-local chiral quark model [125], light-front quark model [108], light-front holographic QCD [126], combined analysis of low and high Q^2 data [107], etc.

In k_T - factorization approach [123], TFFs of π^0 have been calculated using transverse momentum dependent meson wave function. The basic argument given by the authors was as follows: The form factor is found to be suffering from end-point

singularities due to possible dominance of soft region's contributions. This makes it looking incalculable in perturbation theory, though it can be calculated within pQCD if the infrared singularities are handled properly by an appropriate choice of a meson wave function. However, there is no direct interpretation of these results with those obtained using DAs.

In anomaly sum rule approach [124], the TFFs of pseudoscalar mesons have been studied basing on dispersive representation of axial anomaly. This non-perturbative QCD technique has nothing to do with pQCD's factorization technique and so it is valid even if factorization breaks.

Since collinear factorization has been extensively studied and has many applications in the high energy processes, we calculate twist-six corrections to TFF of η, η' using this approach. The meson transition form factor $F_{\gamma\gamma^* \rightarrow M}(q^2, (p-q)^2)$, ($M=\eta, \eta'$) is described by the following matrix element [37, 38, 40, 98, 105]:

$$T_{\mu\nu}(q, p) \equiv i \int d^4x \exp^{-iqx} \langle M(p) | T \{ j_\mu^{em}(x) j_\nu^{em}(0) \} | 0 \rangle = e^2 \epsilon_{\mu\nu\alpha\beta} q^\alpha p^\beta F_{\gamma\gamma^* \rightarrow M}(q^2, (p-q)^2), \quad (3.59)$$

where

$$j_\mu^{em}(x) = \sum_{\psi=u,d,s} e_\psi \bar{\psi}(x) \gamma_\mu \psi(x). \quad (3.60)$$

We consider space-like form factors with $-q^2=Q^2$ being large and $(p-q)^2 \approx 0$. In such a situation we will denote the TFF $F_{\gamma^*\gamma^* \rightarrow M}(q^2, (p-q)^2)$ simply by $F_{\gamma\gamma^* \rightarrow M}(Q^2)$. The correlation function $T_{\mu\nu}(q, p)$ is dominated by light-like distances and therefore amendable to an expansion around the light-cone. The light-cone expansion is performed by integrating out the transverse and "minus" degrees of freedom and leaving the longitudinal momenta of the partons as the required degree of freedom. In practice, the transverse momenta are integrated only up to a cut-off, μ , and momenta below μ are included in DAs. Since s-quark is involved in this case and the masses of η - and η' - mesons are substantially larger compared to pion mass, we introduce lowest order corrections arising due to finite s- quark mass and meson masses along with twist-six corrections to these TFFs. Several light-cone operators of twist-six

can be factorized as a product of two gauge-invariant twist-three operators, or one twist-two and one twist-four operator; placed between vacuum and one meson state, such operators in factorization approximation can be evaluated as a product of quark or gluon condensate and twist-three or twist-two (along with a quark mass) DA. Non-factorizable operators give rise to twist-six multiparton meson DAs. It has been argued that due to conformal symmetry higher Fock states are strongly suppressed at $u \rightarrow 1$ giving negligible contributions [110]. We use this approach to estimate twist-six contributions in this work.

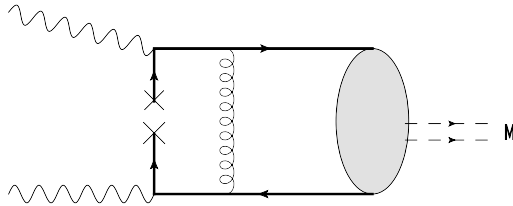


Figure 3.4: Contribution to the TFF from a bilocal pseudoscalar operator along with a quark condensate.

The contribution to the matrix element $T_{\mu\nu}$ from the Feynman diagram shown in Fig.(3.4) comes from bilocal pseudoscalar operator and is given by

$$T_{\mu\nu}^{(3.4)}(q, p)_{(pseudo)} = \frac{8g^2}{9q^2m_\rho^2} \sum_{\psi=u,d,s} e_\psi^2 \frac{1}{m_\psi} \langle \bar{\psi}\psi \rangle \epsilon_{\mu\nu\alpha\beta} q^\alpha p^\beta \int_0^1 du \Phi_{3M}^{(\psi)p}(u) \frac{1}{(q-up)^2}. \quad (3.61)$$

where, u is the momentum fraction of the meson carried by a quark or antiquark. In the above equation we have used vector meson dominance model and replaced $(q-p)^2 \rightarrow m_\rho^2$ in the denominator. We expand the integral in powers of $(1/q^2)$ and retain terms up to order $(1/q^6)$ in this work. The first term in the expansion of expression (3.61) happens to be of $1/q^4$ -type. Neglecting the contributions of the twist-3 three-particle DA, $\Phi_{3\psi}^p(u) = h_\psi$ has been taken [40, 82]. It is to be noted that, in vector meson dominance approximation, the factor $1/m_\rho^2$ is identified with the magnetic susceptibility of the quark condensate [113, 114].

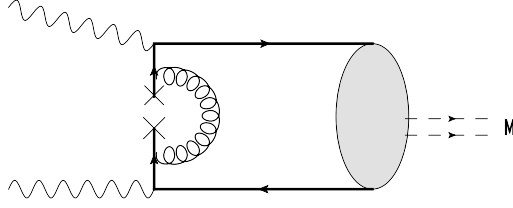


Figure 3.5: Feynman diagram contributing to the TFF through a bilocal tensor operator along with a quark condensate.

The Feynman diagram given by Fig. (3.5) contributes to the matrix element $T_{\mu\nu}$ through a bilocal tensor operator given by,

$$T_{\mu\nu}(q, p)_{(tensor)}^{(3.5)} = \frac{8g^2}{9} \sum_{\psi=u,d,s} e_{\psi}^2 \frac{1}{m_{\psi}} \langle \bar{\psi}\psi \rangle \epsilon_{\mu\nu\alpha\beta} p^{\alpha} \frac{\partial}{\partial q_{\beta}} \int_0^1 du \Phi_{3M}^{(\psi)\sigma}(u) \frac{1}{(q - up)^4}. \quad (3.62)$$

In the considered approximation, $\Phi_{3\psi}^{\sigma}(u) = 6u\bar{u}h_{\psi}$ [40, 82]. The result of the integral is of the type $1/q^6$ in our approximation.

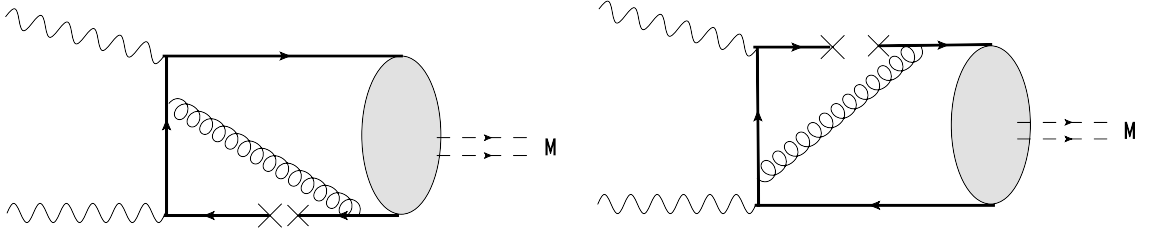


Figure 3.6: Feynman diagrams for TFF obtained by expanding quark propagator close to the light-cone in a background gluon field along with a quark condensate.

The contributions from diagrams corresponding to Fig. (3.6) are obtained by expanding quark propagator close to the light-cone in a background gluon field [83]. Using equation of motion, the covariant derivative of the gluon field strength tensor is converted to a quark-antiquark pair form. This leads to a bilocal tensor operator

yielding

$$T_{\mu\nu}^{(3.6)}(q, p)_{(tensor)} = \frac{g^2}{27} \sum_{\psi=u,d,s} e_\psi^2 \frac{\langle \bar{\psi}\psi \rangle}{m_\psi} \epsilon_{\mu\nu\alpha\beta} p^\alpha \frac{\partial}{\partial q_\beta} \int_0^1 \int_0^1 dudv \times (u\bar{u} - \frac{1}{2}) \left[\frac{u}{q^4(1-uv)^2} + \frac{u}{(q^2uv - p^2(1-uv))^2} \right] \Phi_{3M}^{(\psi)\sigma}(v). \quad (3.63)$$

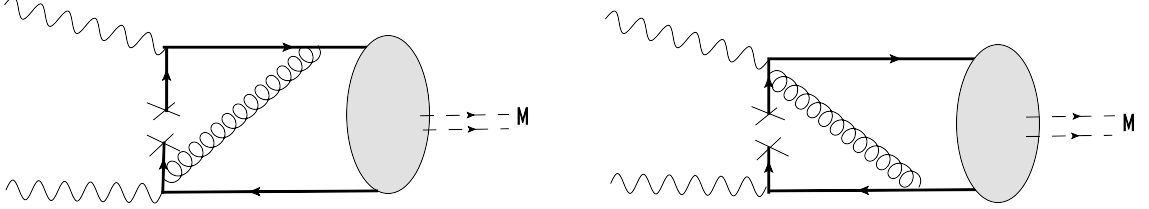


Figure 3.7: Feynman diagrams for TFF obtained from light-cone expansion of the product of two electromagnetic currents.

u in the above equation parameterizes the point where a gluon is emitted from the quark line between 0 and X in the light-cone expansion of the quark propagator whereas v parameterizes the fraction of the meson momentum carried by a quark. Using light-cone expansion of the product of two currents [83] one gets diagrams shown in Fig. (3.7). This results in a tensor-type of bilocal operator and the result can be expressed as

$$T_{\mu\nu}^{(3.7)}(q, p)_{(tensor)} = \frac{g^2}{9} \sum_{\psi=u,d,s} e_\psi^2 \frac{\langle \bar{\psi}\psi \rangle}{m_\psi} \epsilon_{\mu\rho\alpha\beta} p^\alpha \int_{-1}^1 du \int_{-1}^u dv \int_0^1 dw \Phi_{3M}^{(\psi)\sigma}(w) \times \left[\frac{\bar{v}(g_\nu^\beta q^\rho + g_\nu^\rho q^\beta (1 - (1+w+v\bar{w})/2))}{\{q^2\bar{v}\frac{\bar{w}}{2} - p^2(1+w+v\bar{w})/2\}^3} - \frac{(1+u)(g_\nu^\beta q^\rho + g_\nu^\rho q^\beta (1+w-\bar{w}u)/2)}{\{q^2(1+w-\bar{w}u)/2 - p^2\bar{w}(1+u)/2\}^3} \right] \quad (3.64)$$

This is in contradiction to the result obtained in Ref [40] where it has been found to vanish. The result of integral starts with $1/q^4$ -type of term. The diagrams represented by Fig. (3.7) also contribute to axial-vector-type of bilocal operator, albeit with a linear quark mass term in the numerator. This can be retained for s -quark. The corresponding result is

$$T_{\mu\nu}^{(3.7)}(q, p)_{(axial)} = \frac{-2}{3} g^2 e_s^2 m_s f_M^{(s)} \langle \bar{s}s \rangle \epsilon_{\mu\nu\alpha\beta} p^\beta \frac{\partial}{\partial q_\alpha} \int_0^1 du u \bar{u} \int_0^1 dv \Phi_{2M}^{(s)}(v) \times \left[\frac{1}{(q-uvp)^2} + \frac{1}{(q-(v+\bar{v}u)p)^2} \right]. \quad (3.65)$$

This gives $1/q^6$ -type contribution.

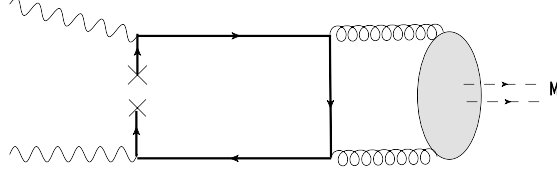


Figure 3.8: Feynman diagram for TFF obtained from expansion of a quark propagator near light-cone involving gluon DA and a quark condensate.

The expansion of a quark propagator near light-cone in the background gluon field also gives rise to a contribution involving gluon DA, as shown in Fig. (3.8); this is linear in quark mass:

$$\begin{aligned}
 T_{\mu\nu}^{(3.8)}(q, p) &= \frac{-g^2 f_M^0}{24^2 \sqrt{3}} e_s m_s \langle \bar{s}s \rangle \epsilon_{\mu\nu\alpha\beta} \bar{n}^\beta \bar{n}_\lambda p_\rho p_\sigma \frac{\partial}{\partial q_\rho} \frac{\partial}{\partial q_\sigma} \frac{\partial}{\partial q_\lambda} \frac{\partial}{\partial q_\alpha} \\
 &\times \int_0^1 du \int_0^u dv \int_0^1 dw \Phi_M^{(g)}(w) (1 - 2\bar{u} - 2v)(u - v)^2 \times \\
 &\left[\frac{1}{(q + p(wu + \bar{w}v))^2} - \frac{1}{(q + p(w\bar{u} + \bar{w}v))^2} \right], \quad (3.66)
 \end{aligned}$$

where \bar{n} is a light-cone constant vector [103, 104]. We estimate this contribution to be of the order of $1/q^8$, and hence, we drop it.

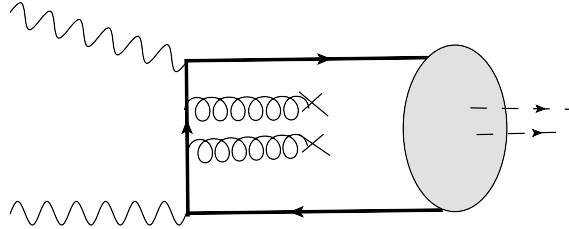


Figure 3.9: A Feynman diagram with a gluon condensate contributing to the TFF. Contribution from this diagram vanishes.

We have also looked into the possibility of contribution from gluon condensate in place of quark condensate times quark mass. However, such contribution arising

from light-cone expansion of quark propagator as well as from product of two currents near light cone, shown in Fig. (3.9), both vanish. Collecting all the contributions from Eqs. (3.61-3.66) and retaining terms only up to order $(1/Q^6)$ in $F_{\gamma\gamma^*\rightarrow\eta^{(\nu)}}(Q^2)$, we get

$$\begin{aligned}
Q^2 F_{\gamma\gamma^*\rightarrow\eta}(Q^2) = & \frac{-16\pi\alpha_s \langle\bar{q}q\rangle}{81} \frac{1}{Q^4} \left[\left\{ \frac{5h_q \cos\phi}{\sqrt{2}m_q} - \frac{\kappa_s}{m_s} h_s \sin\phi \right\} \right. \\
& \times \left\{ \frac{Q^2}{m_\eta^2} - \frac{Q^2}{m_\rho^2} \log\left[\frac{Q^2}{m_\eta^2}\right] - \frac{19}{2} - \frac{2\pi^2}{3} + \frac{7}{2} \log\left[\frac{Q^2}{m_\eta^2}\right] \right. \\
& \quad \left. \left. + \left(-\frac{m_\eta^2}{m_\rho^2} + 4\right) \log\left[\frac{Q^2}{m_\eta^2}\right] - \frac{3}{2} \log^2\left[\frac{Q^2}{m_\eta^2}\right] \right\} \right. \\
& + \left(\frac{9m_s\kappa_s}{\sqrt{3}} \right) \left[\left(f_\eta^0 - \sqrt{2}f_\eta^8 \right) \left(46 - \frac{4\pi^2}{3} - 14 \log\left[\frac{Q^2}{m_\eta^2}\right] + 2 \log^2\left[\frac{Q^2}{m_\eta^2}\right] \right) \right. \\
& \quad \left. + \left\{ f_\eta^0 \left(6B_2^q(\eta_0) L^{\frac{48}{75}} - \frac{B_2^g}{17} L^{\frac{107}{75}} \right) - 6\sqrt{2}f_\eta^8 B_2^q(\eta_8) L^{\frac{2}{3}} \right\} \right. \\
& \quad \left. \left. \times \left\{ \frac{-316}{9} + 2\pi^2 + \frac{31}{6} \log\left[\frac{Q^2}{m_\eta^2}\right] - \frac{1}{2} \log^2\left[\frac{Q^2}{m_\eta^2}\right] \right\} \right] \right], \quad (3.67)
\end{aligned}$$

where $\kappa_s = \langle\bar{s}s\rangle/\langle\bar{q}q\rangle$ (see Appendix for more information on notations). For $Q^2 F_{\gamma\gamma^*\rightarrow\eta'}(Q^2)$, one has to make the substitution ($\cos\phi \rightarrow \sin\phi$, $-\sin\phi \rightarrow \cos\phi$, $m_\eta \rightarrow m_{\eta'}$, $f_\eta^{0,8} \rightarrow f_{\eta'}^{0,8}$) in the above equation. Thus, twist-six contributions for η and η' mesons produce $1/Q^4$ -type correction, same as in the case of pion, given in [40] and like twist-four correction in the case of η, η' [98], but with smaller coefficients.

3.3 Numerical analysis of result

In this work, we use two loop result for running QCD coupling constant with $\Lambda_{QCD}^{(4)}=326$ MeV and four active flavors. In addition, we use constants given in Table.(3.1) at renormalization scale $\mu_0=1$ GeV [85, 98, 104, 105, 117, 127, 128]: Since in this work we are calculating only twist-six corrections to TFFs of η and η' mesons, we shall be using results on leading order and next-to-leading order power corrections arising from lower twists from existing literature. In Table. (3.2), we have displayed the coefficients of $1/Q^4$ and $1/Q^6$ in $F_{\gamma\gamma^*\rightarrow\eta^{(\nu)}}(Q^2)$ for $Q^2 = 5, 10, 50$ GeV². In Table. (3.3), we have displayed the composition of our result for TFFs

Table 3.1: Parameters used in numerical evaluation of the result shown in Eq.(3.67)

Parameter	Numerical Value	Parameter	Numerical Value
$\langle \bar{q}q \rangle$	$-(0.240 \pm 0.010 \text{ GeV})^3$	$B_2^q(\eta_0)=B_2^q(\eta_8)$	0.115 ± 0.035
κ_s	(0.8 ± 0.1)	$B_{2,g}$	18 ± 2
m_q	$(4.5 \pm 0.5)\text{MeV}$	h_q	$0.0015 \pm 0.004 \text{ GeV}^3$
m_s	$(100 \pm 10)\text{MeV}$	h_s	$0.087 \pm 0.006 \text{ GeV}^3$
ϕ	$39.3^\circ \pm 1.0^\circ$	m_ρ	0.77 GeV
f_q	$(1.07 \pm 0.02)f_\pi$	Γ_ρ	0
f_s	$(1.34 \pm 0.06)f_\pi$		

as ratios of different contributing Lorentz structures to the total twist-six result. It demonstrates as to how the cancellation among the pseudoscalar and tensor structures results in a small value of overall result.

On the Uncertainties of h_q

Since h_q has been found to influence the result on twist-six contribution considerably, it is worth discussing the origin of its uncertainties. If the errors of $f_{q,s}$ and ϕ are treated as uncorrelated, then expression(3.52) gives $h_q=(0.0015 \pm 0.004) \text{ GeV}^3$ [84], $\sim 270\%$ uncertainty. However, QCD-sum-rule estimate given in Ref. [127] yields $h_q=(0.0025 \pm 0.0009) \text{ GeV}^3$. In Ref. [85], the authors have considered $\frac{h_q}{(2m_q)}$ which normalizes twist-three DAs of η_q . Working to leading order in chiral expansion they set $\frac{h_q}{(2m_q)}=f_q B_0$ with $B_0= m_\pi^2/(2m_q)=-2\langle 0 | \bar{q}q | 0 \rangle/f_\pi^2$. With the uncertainty in $\langle \bar{q}q \rangle$ and f_q as given above and $m_q=(4-5) \text{ MeV}$, one finds $h_q=(0.0021 \pm 0.0005) \text{ GeV}^3$. Another approximate numerical estimate of h_q can be given using the octet-singlet basis of $\eta - \eta'$ system. In Ref. [129], $\mu_\eta=3m_\eta^2/(m_u + m_d + 4m_s)$, chirally enhanced factor, has been introduced in the matrix element of octet pseudoscalar quark current between vacuum and one- η state assuming it to be a pure octet in analogy with μ_π and μ_K . Similarly, in Ref. [103], $\mu_{\eta'}=3m_{\eta'}^2/(2m_u + 2m_d + 2m_s)$ has been introduced in the matrix element of singlet pseudoscalar quark current between vacuum and one- η' state assuming it to be a pure singlet state. Writing

these matrix elements in both quark-flavor as well as octet-singlet basis one gets

$$\frac{h_q \cos \phi}{\sqrt{12}m_q} + \frac{h_s \sin \phi}{\sqrt{6}m_s} = f_\eta^8 \mu_\eta, \quad (3.68)$$

$$\frac{h_q \sin \phi}{\sqrt{6}m_q} + \frac{h_s \cos \phi}{\sqrt{12}m_s} = f_{\eta'}^0 \mu_{\eta'}. \quad (3.69)$$

These equations can be solved together to estimate h_q in an approximate way since η and η' are not simply octet and singlet states respectively as treated in this derivation. Taking the numerical values of f_η^8 and $f_{\eta'}^0$, as well as (for the sake of consistency) the quark masses from Ref. [127], we estimate $h_q \simeq 0.0057 GeV^3$. This barely touches the upper limit of the first estimate given in this paragraph.

The plots

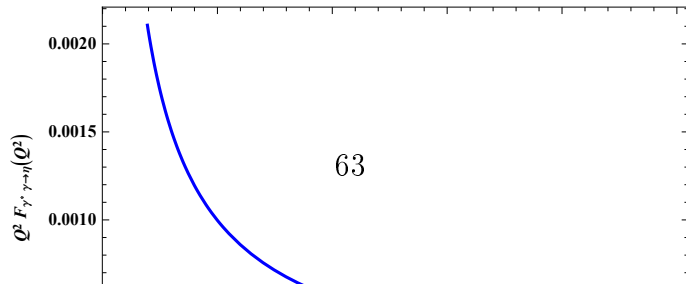
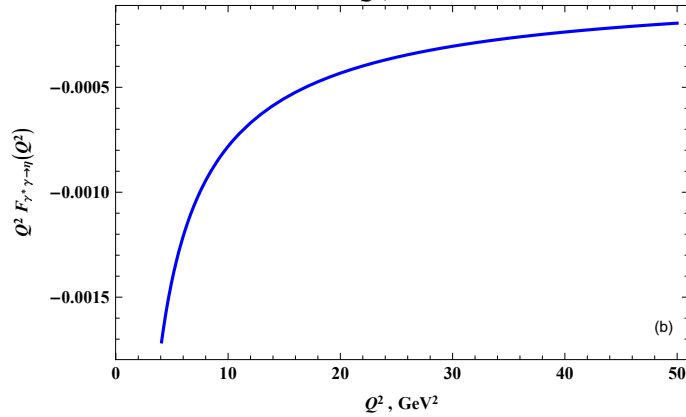
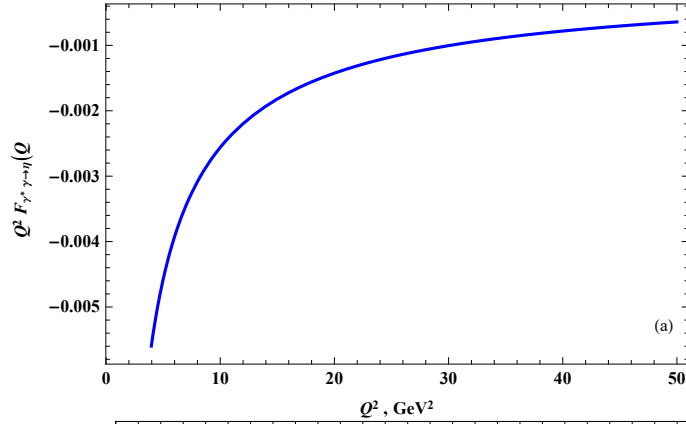
In Figs. (3.10) and (3.15), we have shown our result for twist-6 correction to the TFF $F_{\gamma\gamma^* \rightarrow \eta^{(\prime)}}(Q^2)$ for $h_q=0.0055, 0.0015$ and -0.0025 which covers the range obtained in the first estimate. In Tables. (3.2) and (3.3) as well as later in Figs. (3.11) and (3.14), we have picked up one $h_q \simeq 0.0020 GeV^3$ which lies in more narrow ranges given in the second and third estimates. For the argument of the running QCD coupling constant, we use frequently used scale $\mu^2=Q^2$. In Figs. (3.11) and (3.14), we have compared our result for twist-six correction to $F_{\gamma\gamma^* \rightarrow \eta^{(\prime)}}(Q^2)$ with the result for twist-four correction to the same from Ref. [98]. In Ref. [46], TFFs $F_{\gamma\gamma^* \rightarrow \eta^{(\prime)}}(Q^2)$ have been calculated to leading twist accuracy and NLO of perturbative QCD with Gegenbauer coefficients of order-2 fixed with an aim to fit the data. In Figs. (3.12) and (3.16), we have superimposed our results of twist-six corrections for TFFs $F_{\gamma\gamma^* \rightarrow \eta^{(\prime)}}(Q^2)$ on the corresponding results obtained in Ref. [46]. The shaded area shows the uncertainty in our result due to uncertainty in various input parameters, as given above in this section, and has been shown separately in Figs.3.12(a) and 3.16(a) for clarity.

Table 3.2: Coefficients of $\frac{1}{Q^4}$ and $\frac{1}{Q^6}$ in our result for the TFFs $F_{\gamma\gamma^*\rightarrow\eta^{(\prime)}}(Q^2)$ at different momenta. Parameters used for evaluation: $\langle\bar{q}q\rangle = (-0.24)^3\text{GeV}^3$, $\kappa_s = \frac{\langle\bar{s}s\rangle}{\langle\bar{q}q\rangle} = 0.8$, $\phi = 40.3^\circ$, $h_q = 0.0020\text{GeV}^3$, $h_s = 0.087\text{GeV}^3$, $f_q = 1.07f_\pi$, $f_s = 1.34f_\pi$, $m_q = 4.5\text{MeV}$, $m_s = 100\text{MeV}$, $B_2^q(\eta_0) = B_2^q(\eta_8) = 0.15$, $B_2^g = 16$.

Q^2	Coefficient of $\frac{1}{Q^4}$		Coefficient of $\frac{1}{Q^6}$	
	η	η'	η	η'
5	-0.0048	-0.0103	-0.0220	-0.0287
10	-0.0075	-0.0148	-0.0266	-0.0357
50	-0.0118	-0.0218	-0.0445	-0.0580

Table 3.3: Ratios of different Lorentz structures to the total twist-six result for the TFFs $F_{\gamma\gamma^*\rightarrow\eta^{(\prime)}}(Q^2)$ at different momenta. Parameters used for this evaluation are the same as those used in Table.3.2.

Q^2	η			η'		
	$\frac{F_{pseudo-6}}{F_{twist-6}}$	$\frac{F_{axial-6}}{F_{twist-6}}$	$\frac{F_{tensor-6}}{F_{twist-6}}$	$\frac{F_{pseudo-6}}{F_{twist-6}}$	$\frac{F_{axial-6}}{F_{twist-6}}$	$\frac{F_{tensor-6}}{F_{twist-6}}$
5	1.850	0.020	-0.870	1.230	-0.041	-0.189
10	1.742	0.010	-0.752	1.205	-0.011	-0.194
50	1.524	0.002	-0.526	1.153	-0.001	-0.152



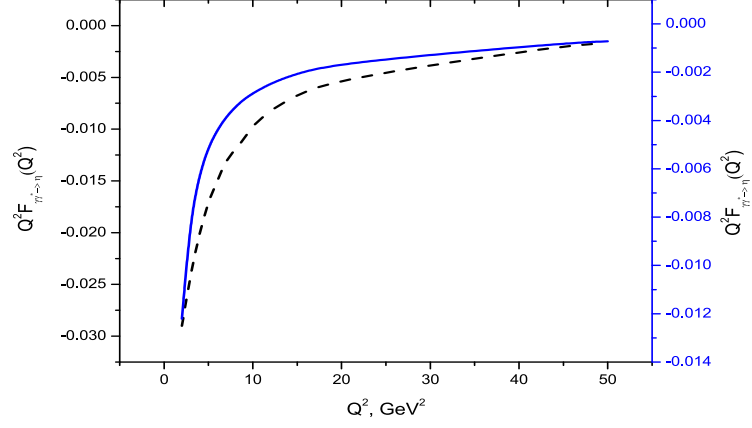


Figure 3.11: Comparison of our result for twist-six correction to the TFF $F_{\gamma\gamma^*\rightarrow\eta}(Q^2)$ (solid line, right scale) with twist-four correction [98] to the same (dashed line, left scale). Parameters used are the same as used in Table .3.2

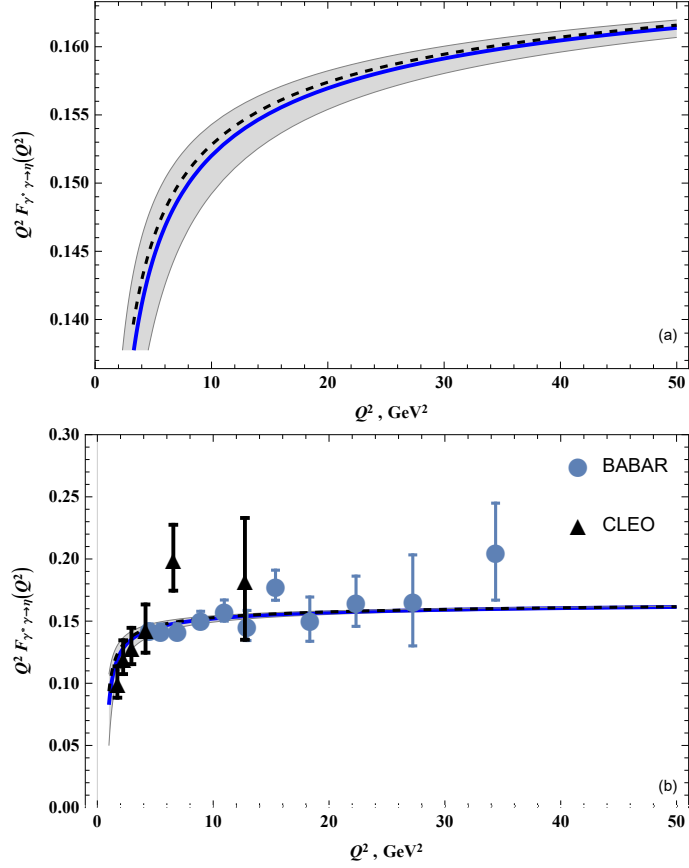


Figure 3.12: Plots of our result for twist-six correction (solid lines) superimposed on the result obtained in Ref.[46] (a)(dashed line, plotted by us) for the TFF $F_{\gamma\gamma^*\rightarrow\eta}(Q^2)$. The shaded area corresponds to the uncertainty in our result due to the variation of the input parameters as given in the text. In (b) the same results are compared with data from Refs. [93, 96].

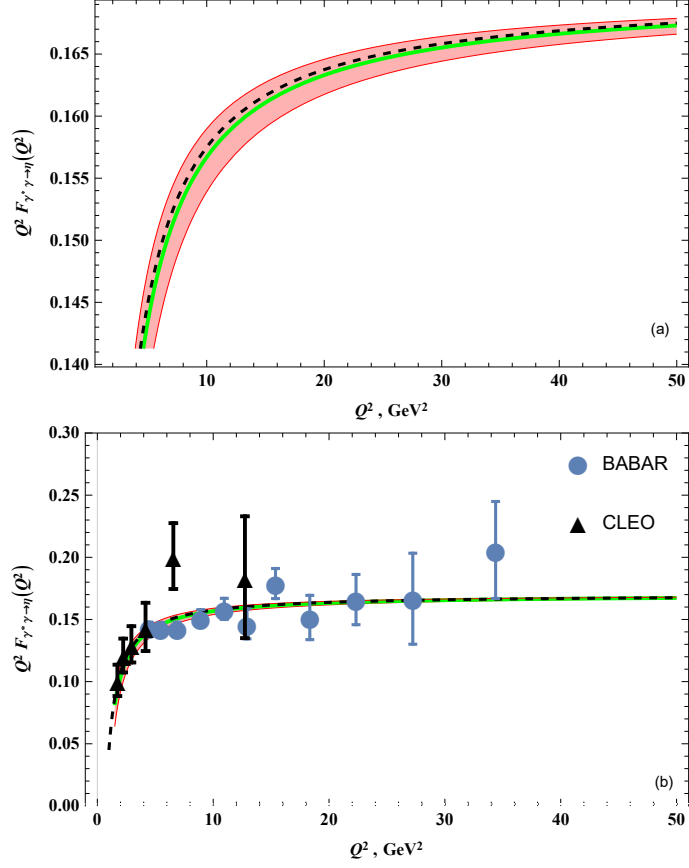


Figure 3.13: Plots of our result for twist-six correction (solid lines) superimposed on the result obtained in Ref.[98] (a)(dashed line, plotted by us) for the TFF $F_{\gamma\gamma^*\to\eta}(Q^2)$. The shaded area corresponds to the uncertainty in our result due to the variation of the input parameters as given in the text. In (b) the same results are compared with the data from Refs. [93, 96].

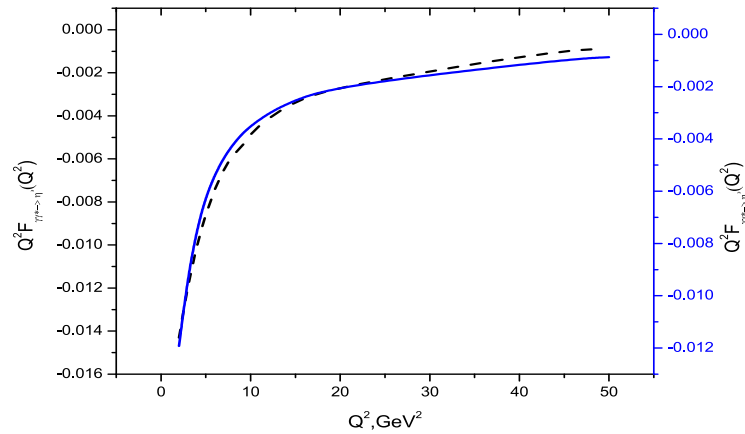


Figure 3.14: Comparison of our result for twist-six correction to the TFF $F_{\gamma\gamma^*\to\eta'}(Q^2)$ (solid line, right scale) with twist-four correction [98] to the same (dashed line, left scale). Parameters used are the same as used in Table. 3.2.

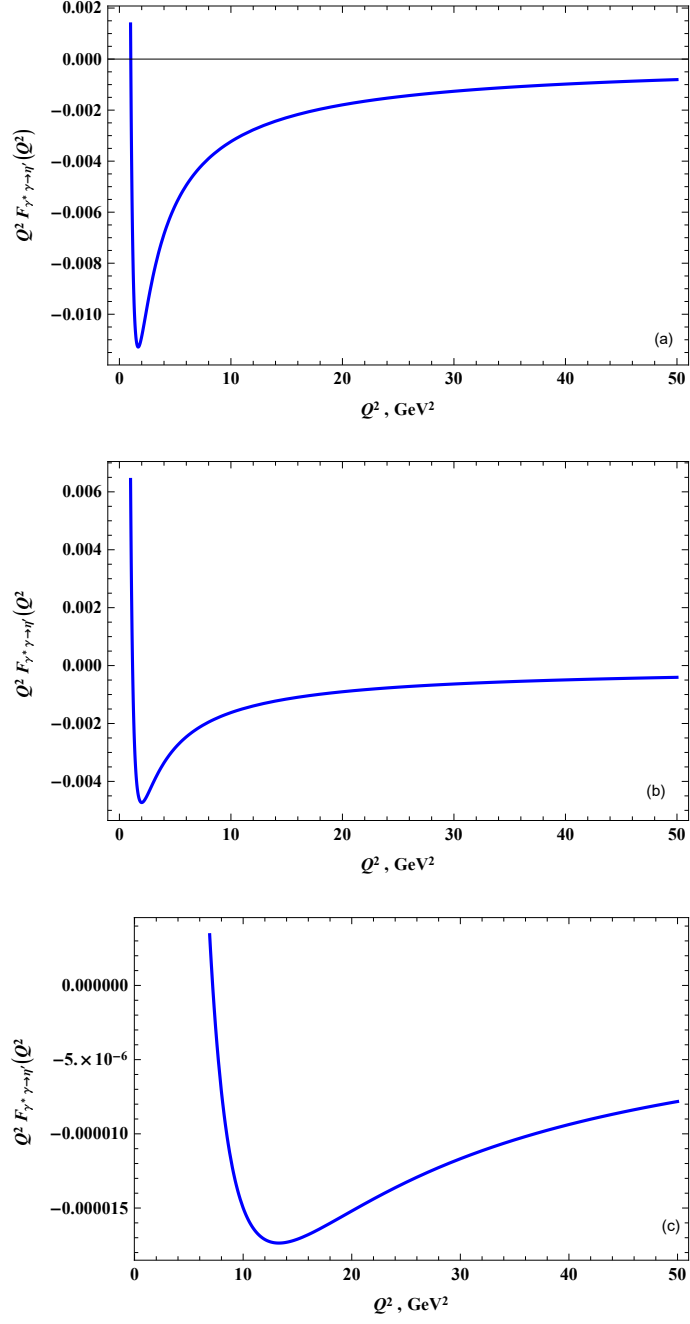


Figure 3.15: Plots of our result for twist-six correction to the TFF $F_{\gamma\gamma^*\rightarrow\eta'}(Q^2)$ for $h_q=0.0055$ (a), 0.0015 (b) and -0.0025 (c).

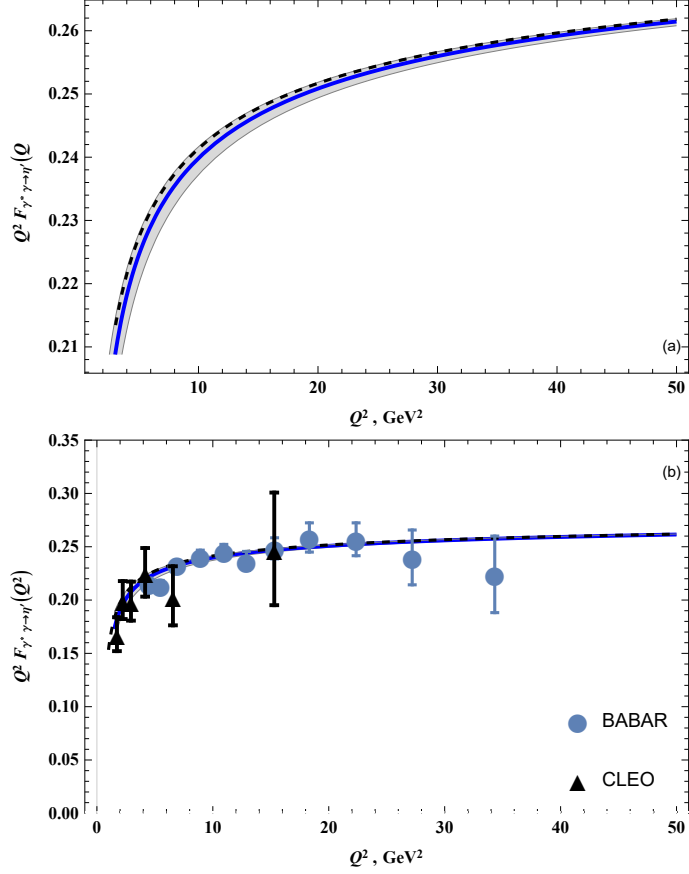


Figure 3.16: Plots of our result for twist-six correction (solid lines) superimposed on the result obtained in Ref.[46](a) (dashed line, plotted by us) for the TFF $F_{\gamma\gamma^*\rightarrow\eta'}(Q^2)$. The shaded area corresponds to the uncertainty in our result due to the variation of the input parameters as given in the text. In (b) the same results are compared with the data from Refs. [93, 96].

In Figs. (3.12) and (3.16), we compare this combination of results with the data from Refs. [93, 96]. Results on TFFs for η and η' mesons obtained in Ref. [98] include NLO analysis of perturbative corrections, charm-quark contribution, SU(3)-flavor breaking effects and the axial anomaly contributions to the power-suppressed twist-4 DAs. In Figs. (3.13)(a) and (3.17)(a), we have shown the results obtained by superimposing our results on those obtained in Ref. [98] for a specific set of parameters. Again the shaded area shows the uncertainty in our results only due to uncertainty in various input parameters as given above in this section. Figs. (3.13)(b) and (3.17)(b) show the comparison of this combination with data points.

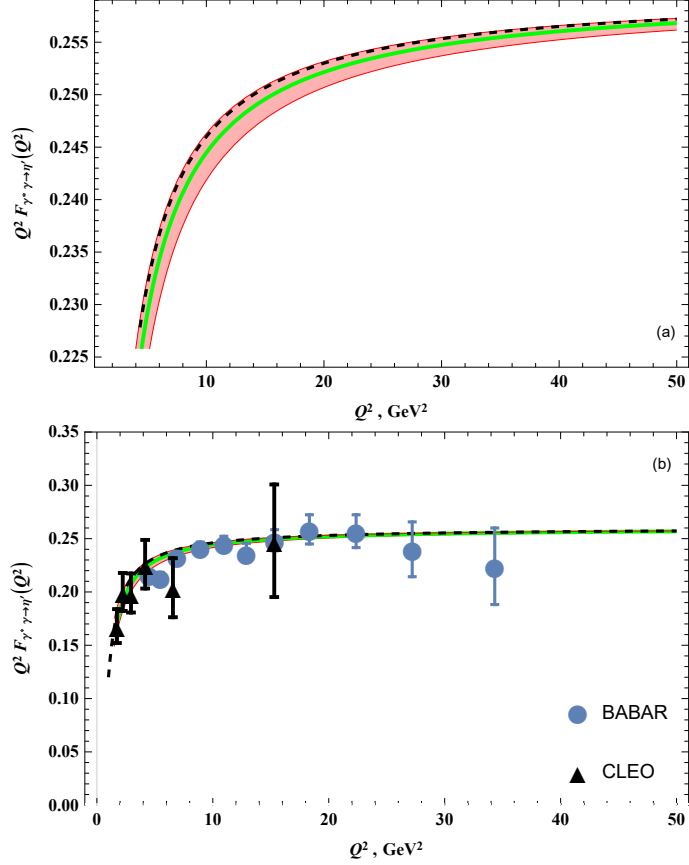


Figure 3.17: Plots of our result for twist-six correction (solid lines) superimposed on the result obtained in Ref. [98](a) (dashed line, plotted by us) for the TFF $F_{\gamma^* \rightarrow \eta'}(Q^2)$. The shaded area corresponds to the uncertainty in our result due to the variation of the input parameters as given in the text. In (b) the same results are compared with the data from Refs. [93, 96]

3.4 Summary and conclusion

Our results on twist-six corrections to TFFs for η and η' mesons start with $1/Q^4$ -type of terms, as is the case for twist-four corrections [98], but with a smaller coefficient. For this calculation, we have considered a subset of twist-six operators which can be factorized as a product of two gauge invariant twist-three operators or one twist-two and one twist-four operator. Our general framework is to use the light-cone expansion of the product of two currents or light-cone expansion of a quark propagator. In addition, we have also used Feynman diagrams which are not accounted for by light-cone expansion. We found that the gluon condensate along with twist-two

DA does not contribute to TFFs. We also observed that the contribution from the meson DA with two valance gluons, being a special case for η and η' mesons, has a higher order term in momentum expansion, and hence has been dropped in our approach. Nevertheless, gluon DA contribution appears due to quark-gluon mixing and renormalization group evolution. Non-factorizable operators are expected to give negligible contribution [110]. We have used vector-dominance model to regulate the result when one of the quark lines goes to the mass-shell. Twist expansion provides a systematic way to calculate higher order power corrections to exclusive processes, our endeavor is to estimate contribution arising from twist-six operators to TFFs of η and η' mesons. Since the mesons involved are not simply Goldstone bosons due to their anomalous masses, we have included their masses as well as the s-quark mass (linear) in our result. We found that h_q , which is the first term in Gegenbauer expansion of twist-three DA of pseudoscalar-type, introduces considerable uncertainty if it is not well constrained. We observed that twist-six contribution is a couple of times smaller in magnitude than twist-four contribution for the η meson, but for η' meson these two contributions are comparable. As far as light-cone sum rules are concerned, we found that they introduce less than 10% modification for twist-four operators for $Q^2 > 7\text{GeV}^2$ in [98] and around 25% modification for twist-six operators in [40]. In our case, they may modify the result by up to 20% due to higher Borel mass and higher continuum threshold. This will be a small change to the total result for TFFs $F_{\gamma\gamma^*\rightarrow\eta^{(\prime)}}(Q^2)$. We feel that any further higher twist correction will make insignificant improvement in the total result for TFFs. Constraining parameters, such as h_q , is better called for. Including few more terms in the expansion of lower-twist DAs, taking non-valance quark(gluon) contribution and taking into account the k_T -corrections when $Q^2 \sim$ a few GeV^2 are other steps which can be taken to improve theoretical results in this approach.

3.5 Appendix

Here, we give few important steps for calculation of two Feynman diagrams given by Figs (3.4) and (3.6). The method involved in calculating these two diagrams are quite different from each other and other diagrams follow from either of these methods. In pQCD, the time ordered product of two electromagnetic current is written as,

$$T\{j_\mu^{em}(x)j_\nu^{em}(0)\} = -e_q^2 \frac{g^2}{2} \int d^4x_1 d^4x_2 T\{A_\rho^a(x_1)A_\lambda^b(x_2) [\bar{q}(x_1)\gamma^\rho t^a q(x_1)\bar{q}(x)\gamma_\mu q(x)\bar{q}(0)\gamma_\nu q(0)\bar{q}(x_2)\gamma^\lambda t^b q(x_2)]\}, \quad (3.70)$$

Here, one has to do all possible contractions leaving two non-local operators uncontracted. Gluon fields enter through S-matrix which encodes QCD interaction Lagrangian given by,

$$S = T \exp[i \int d^4x \mathcal{L}_{int}^0(x)], \quad (3.71)$$

where, $\mathcal{L}_{int}^0(x) = g\bar{q}A^a t^a q$. Eq. (3.70) takes the form,

$$T\{j_\mu^{em}(x)j_\nu^{em}(0)\} = -e_q^2 \frac{g^2}{2} \int d^4x_1 \int d^4x_2 D_{\rho\lambda}^{ab}(x_1 - x_2) [\bar{q}(x_1)\gamma^\rho t^a S(x_1 - x)\gamma_\mu S(x)\gamma_\nu S(-x_2)\gamma^\lambda t^b q(x_2) + \bar{q}(x_2)\gamma^\lambda t^b S(x_2 - x)\gamma_\mu S(x)S(-x_1)\gamma_\nu \gamma^\rho t^a q(x_1)] + \dots (x \leftrightarrow 0, \mu \leftrightarrow \nu), \quad (3.72)$$

The product of operators which are not contracted is written as,

$$\psi_a^\alpha(x)\bar{\psi}_b^\beta(0) = \frac{\delta^{ab}}{12} [(\gamma^\mu \gamma_5)^{\alpha\beta} \bar{\psi}(0)\gamma_\mu \gamma_5 \psi(x) + i\gamma_5^{\alpha\beta} \bar{\psi}(0)i\gamma_5 \psi(x) - \gamma_5(\sigma^{\mu\nu})^{\alpha\beta} \bar{\psi}(0)\gamma_5 \sigma_{\mu\nu} \psi(x)]. \quad (3.73)$$

The matrix element of operators on R.H.S between vacuum and one-meson state is parameterized by the corresponding distribution amplitude. One of the quark propagator, $S(x)$, is written in terms of light-cone expansion as given by Eq. (2.29).

Other two quark propagators are written as,

$$S(x)^{ab} = \int \frac{d^4p}{(2\pi)^4} e^{-ip \cdot x} \tilde{S}(p)^{ab}, \quad (3.74)$$

where $\tilde{S}(p)^{ab} = \delta^{ab} \frac{i}{\not{p} - m + i\epsilon}$. Gluon propagator reads,

$$D_{ab}^{\mu\nu}(x) = \frac{1}{(2\pi)^4} \int d^4k e^{-ik \cdot x} \tilde{D}_{ab}^{\mu\nu}(k), \quad (3.75)$$

where, $\tilde{D}_{ab}^{\mu\nu}(k) = -i\delta^{ab}(\frac{g^{\mu\nu} + \xi k^\mu k^\nu / (k^2 + i0)}{k^2 + i0})$. As shown in Eq.(3.59), the next step is to take fourier transform of the expectation value of the time-ordered product of two electromagnetic currents between vacuum and one-meson state. After few simplifications and performing necessary integrations, the calculation finally reduces to form given by Eq.(3.61).

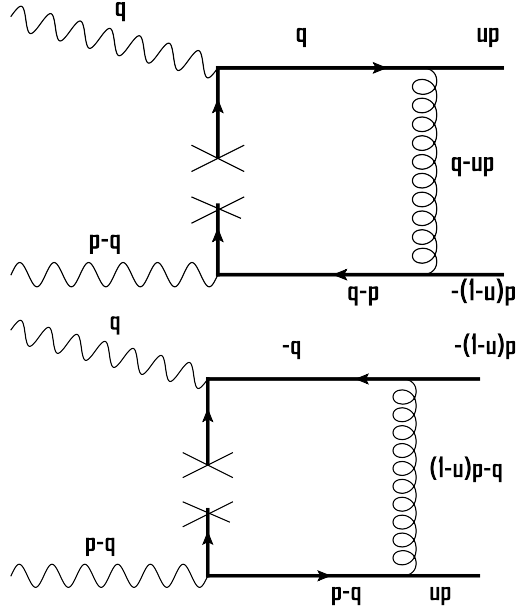


Figure 3.18: Four-momenta flowing through the Feynman graphs is conserved at each vertex.

To calculate diagram (3.6), the light-cone expansion of quark propagator reads [83],

$$i\psi(0)\bar{\psi}(x) = i\frac{\Gamma(\frac{d}{2} - 2)}{16\pi^2(-x^2)^{d/2-2}} \int du(\bar{u}u - 1/2)D^\mu G_{\mu\nu}(\bar{u}x)\gamma^\nu + \dots \quad (3.76)$$

and

$$D^\lambda G_{\lambda\rho} = -g_s T^a \bar{\psi} \gamma_\rho T^a \psi, \quad (3.77)$$

is a QCD equation of motion.

$$\Gamma(-\epsilon)(-x^2)^\epsilon = \Gamma(-\epsilon) + \epsilon\Gamma(-\epsilon) \log(-x^2) \rightarrow -\log(-x^2), \quad (3.78)$$

$$i\psi(0)\bar{\psi}(x) = \frac{g_s^2}{16\pi^2} \log(-x^2) t_{ij}^a \int_0^1 du(\bar{u}u - 1/2) \bar{\psi}(\bar{u}x) \gamma_\nu t^a \psi(\bar{u}x) \gamma^\nu + \dots \quad (3.79)$$

Now, we want to calculate

$$\langle M(p) | T\{\bar{\psi}^i(0)\gamma_\nu\psi(0)^i\bar{\psi}(x)^j\gamma_\mu\psi(x)^j\} | 0\rangle, \quad (3.80)$$

In above equation, we can contract $\psi(0)^i \bar{\psi}(x)^j$ and leave two other field-operators as it is and we can contract $\bar{\psi}(0)^i \psi(x)^j$ and leave the other two. All these possibilities have to be taken into account while calculating the matrix element. By substituting Eq.(3.79) in above equation, we get,

$$\begin{aligned} \langle M(p) | T\{\bar{\psi}^i(0)\gamma_\nu\psi(0)^i\bar{\psi}(x)^j\gamma_\mu\psi(x)^j\} | 0\rangle &= \frac{g_s^2}{16\pi^2} \log(-x^2)t_{ij}^a \int_0^1 du(\bar{u}u - 1/2) \times \\ &\langle M(p) | T\{\bar{\psi}^i(0)\gamma_\nu(t^a)_{ij}\bar{\psi}(\bar{u}x)\gamma_\rho t^a\psi(\bar{u}x)\gamma^\rho\gamma_\mu\psi(x)^j\} | 0\rangle, \end{aligned} \quad (3.81)$$

$$\begin{aligned} \langle M(p) | T\{\bar{\psi}(0)\gamma_\nu(t^a)\bar{\psi}(\bar{u}x)\gamma_\rho t^a\psi(\bar{u}x)\gamma^\rho\gamma_\mu\psi(x)\} | 0\rangle &= -(\gamma_\nu t^a \gamma_\rho \gamma_\mu)_{ij} (\gamma^\rho t^a)_{kl} \times \\ &\{\langle M(p) | T\{\bar{\psi}(0)_i\psi(\bar{u}x)_l\} | 0\rangle \langle 0 | T\{\bar{\psi}(\bar{u}x)_k\psi(x)_j\} | 0\rangle + \\ &\langle 0 | T\{\bar{\psi}(0)_i\psi(\bar{u}x)_l\} | 0\rangle \langle M(p) | T\{\bar{\psi}(\bar{u}x)_k\psi(x)_j\} | 0\rangle\}. \end{aligned} \quad (3.82)$$

In above equation, for quark propagators, light-cone expansion given by Eq.(2.29) has been used and other operators are first written as given by Eq.(3.73) and then the matrix element of operators between vacuum and one-meson state is parameterized by the distribution amplitude. After performing necessary steps, the Eq. (3.82) reduces to Eq.(3.63).